INL/CON-23-75007-Revision-1

Development of an Improved RELAP5-3D Model for the High Temperature Test Facility

November 2024

Robert Forrester Kile, Aaron S Epiney

Changing the World's Energy Future

Idaho National Laboratory

INL is a U.S. Department of Energy National Laboratory operated by Battelle Energy Alliance, LLC

INL/CON-23-75007-Revision-1

Development of an Improved RELAP5-3D Model for the High Temperature Test Facility

Robert Forrester Kile, Aaron S Epiney

November 2024

Idaho National Laboratory
Idaho Falls, Idaho 83415

http://www.inl.gov

Prepared for the
U.S. Department of Energy
Under DOE Idaho Operations Office
Contract DE-AC07-05ID14517

Development of an Improved RELAP5-3D Model for the High Temperature Test Facility

Robert F. Kile and Aaron S. Epiney
Idaho National Laboratory, Idaho Falls, ID, USA
Corresponding Address
robert.kile@inl.gov; aaron.epiney@inl.gov

[leave space for DOI, which will be inserted by ANS]

ABSTRACT

High-temperature gas-cooled reactors (HTGRs) are rapidly approaching deployment. Confidence in transient analysis of these systems requires modeling and simulation tools that have been validated against data relevant to HTGR conditions. The High Temperature Test Facility (HTTF) is an integral effects thermal hydraulics test facility for prismatic HTGRs. In spring and summer of 2019, HTTF was used for a series of experiments that now serve as the basis for the Organization of Economic Cooperation and Development / Nuclear Energy Agency Thermal Hydraulic Code Validation Benchmark for High Temperature Gas-Cooled Reactors using HTTF Data (HTGR T/H Benchmark).

Previous analyses as part of the HTGR T/H benchmark used a RELAP5-3D model developed at Idaho National Laboratory (INL) and demonstrated an ability to reproduce trends in the measured data but difficulties reproducing experimental values within their uncertainty. These difficulties were largely attributed to assumptions made during the development of the initial RELAP5-3D model, which predated the HTTF experiments. A significant cause of difficulty reproducing the measured temperatures may be the radial nodalization of the previous RELAP5-3D model.

In this paper, we present a new RELAP5-3D model of HTTF with finer radial nodalization built to assess the impact of radial heat transfer. We describe the new model and compare it against the old one at full-power steady state and for the pressurized conduction cooldown (PCC) transient. These analyses are based on the code-to-code comparison exercise for the PCC problem of the HTGR T/H benchmark. We compare maximum block temperature as the primary figure of merit and include discussion on intracore natural circulation.

KEYWORDS
RELAP5-3D, validation, benchmark, HTTF, HTGR

1. INTRODUCTION

High-temperature gas-cooled reactors (HTGRs) are an advanced reactor concept of interest due to their high degree of inherent safety and their ability to expand the mission of nuclear energy beyond electricity generation. This is made possible by the high coolant outlet temperatures common in HTGR designs. HTGRs are being considered for deployment at power levels ranging from a few megawatts to hundreds of megawatts. In 2017, the US Department of Energy (DOE)'s Advanced Demonstration and Test Reactor Options Study identified HTGRs as having a technology readiness level sufficient to support commercial deployment by the early 2030s [1]. The High Temperature Test Facility (HTTF) is an integral effects

thermal hydraulics (TH) test facility located at Oregon State University (OSU) that was used in a set of experiments in spring and summer of 2019 that provides validation data for prismatic HTGR TH modeling. To support code validation efforts and accelerate the deployment of HTGRs, the DOE's Advanced Reactor Technologies – Gas-cooled Reactor (ART-GCR) campaign is supporting the development of the Thermal Hydraulics Code Validation Benchmark for High Temperature Gas-Cooled Reactors using HTTF Data (HTGR T/H Benchmark). This benchmark is based on three HTTF experiments [2]. Most RELAP5-3D modeling of HTTF has used a model developed at Idaho National Laboratory (INL) from 2015-2018. That model is described in depth in reference [3]. Several studies using the existing model from INL were able to reproduce the trends in HTTF data but an inability to reproduce measured values [4-8]. In the PG-26 experiment, differences between RELAP5-3D predictions and experimental data have primarily been attributed to uncertainties in the state of the facility during the experiment [4, 6]. Differences between RELAP5-3D predictions and experimental temperatures in experiments PG-27 and PG-29 are hypothesized to be the result of model discretization and simplifications that were made during the development of the existing INL model which led to a mismatch in power density between the experiments and the models [9]. To test this hypothesis, we developed an improved RELAP5-3D model that better captures local temperature and power distributions compared to the previous model. In this paper, we first provide background on the old model. We then provide a detailed description of the new model. Finally, we compare temperatures from the new model and old model during a 2.2 MW steady state, and a pressurized conduction cooldown (PCC). Work comparing the new model to experimental data is ongoing and will be presented in a future paper.

The results contained in this paper represent initial analysis to assess the performance of the new model prior to validation work. The good agreement between the new and legacy models that we show in this paper provides confidence that we can move forward with the new model for validation work.

1.1 Review of the Legacy INL HTTF RELAP5-3D Model

The RELAP5-3D model of HTTF that has been used by INL [4, 5], the University of Tennessee [6, 8], and OSU [7] is the model described in reference [3]. A radial nodalization diagram of that model can be seen in Figure 1. The inner (central) reflector is modeled with three rings, with the middle cylinder containing the six inner reflector coolant channels. The model of the core region is divided into three rings as well, each containing heater rods, coolant channels, and core block material. These are referred to as the inner, middle, and outer core regions. The side reflector shown in Figure 1 is referred to in this work as the outer reflector. The outer reflector is also divided into three regions in the model with the middle region containing the 36 outer reflector coolant channels. A small gap is modeled between the outer and permanent reflector. Heat is transferred across this gap by radiation between the outer and permanent reflectors. The permanent reflector is modeled using a single heat structure. Its inside is connected to a helium gap between the outer and permanent reflectors. On the outside, this heat structure is connected to a gap between the permanent reflector and core barrel. Heat is transferred across this gap using radiation heat transfer.

The inner reflector, core region, and outer reflector of the facility are composed of an aluminum oxide-based ceramic with a thermal conductivity on the order of 2-5 W/m-K [10]. This was done to create HTGR-relevant temperatures despite the much lower power density of HTTF compared to the General Atomics Modular High-Temperature Gas Reactor (MHTGR). The power in HTTF is approximately $1/160^{th}$ the power of MHTGR, and the volume is $1/64^{th}$ the volume of MHTGR. The permanent reflector is made of a silicon carbide-based ceramic called Shot-Tech SiC 80. Thermal conductivity, specific heat, and emissivity data for the Shot-Tech were not available, so Bayless used properties of a ceramic with a similar chemical composition to the Shot-Tech when developing the existing model [3].

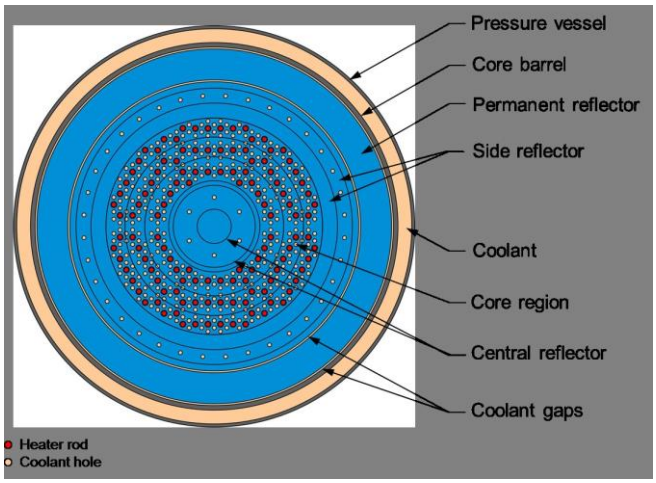

Figure 1. Radial nodalization diagram of the existing INL RELAP-53D model. Reproduced from [3].

The inner and outer core regions contain coolant channels of three different diameters, as shown in Table I. The inner region contains 56 heater rods at various radial positions. The middle region has only large coolant holes and has 72 heater rods. The outer region contains 82 heater rods. In each region of the core, the heater rods are represented using a single heat structure with surface area terms set to capture the correct number of heater rods. In the inner and outer rings, the flow area from all coolant channels is preserved, but the coolant channel diameter was adjusted to match the core pressure drop of a standalone model that models the 3 different-sized coolant channels separately [3].

Table I. Coolant channel information for the whole core.

	Small Channels	Medium Channels	Large Channels
Diameter (cm)	0.9525	1.2700	1.5875
Number of Channels	96	96	324

Radial conduction is a significant heat transfer mechanism in HTGRs and is one of the primary heat removal mechanisms during transients in which forced flow of the coolant is lost. In this model, radial conduction is accomplished through three conduction enclosures. The first enclosure represents conduction in the inner reflector. The second enclosure represents conduction in the core and connects to the reflectors. The third enclosure represents conduction in the outer reflector.

The heater rods are not connected to any hydrodynamic components. They communicate with the core blocks via radiation heat transfer. The helium gap between the heater rods and the core blocks is also modeled, but the gap communicates only with the outside of the core blocks. The inside surface of the core blocks is connected to the pipes representing the coolant channels.

The legacy model includes the entire primary coolant circuit, the steam generator, and the reactor cavity cooling system (RCCS), but some of the analyses in the literature use a simplified model that neglects the primary and secondary circuits, modeling only the RCCS and the contents of the reactor vessel [7, 9]. The new model presented in this work models only the RCCS and the contents of the reactor vessel, so the primary and secondary circuits are neglected outside the reactor vessel. The results presented in this paper that use the legacy model also use a version that neglects the primary and secondary circuits. The coolant

circuits are neglected because including them requires significantly more run time and does not improve the fidelity of the heat transfer behavior in the core itself.

2. DEVELOPMENT OF THE NEW MODEL

The development of this model is broken up into development of the hydrodynamic components and development of the heat structures. All the heat structures within the core barrel and between the upper and lower plena were redefined in the new model. As hydrodynamic components were built, we tested the model against the legacy model without heat generation, to provide confidence that our hydrodynamic components were built properly.

2.1. Hydrodynamic components

The basic unit cell used to derive the model geometry in the core is a hexagon centered on the heater rod with coolant channels as its borders. This unit cell can be seen in Figure 2 (right). Each vertex of the hexagon is equal to 1/3 of a coolant channel. The hole labeled “heater rod” is a combination of the heater rod and the helium gap that separates the heater rod from the block. The coolant, block, and heater hole volume fractions in the unit cell from Figure 2 are used to generate a unit cell for the RELAP5-3D model. Figure 2 (left) also shows a view of part of the core with three different-colored hexagons. Applying the unit cell from the right of Figure 2 to the core view on the left, there are a total of 9 “rings” containing heater rods. There are 2 additional “rings”, one at the inner edge of the core and one at the outer edge of the core. Each “ring” contains multiple hexagonal unit cells, and the flow area of the ring is equal to the flow area of the coolant channels per unit cell multiplied by the number of unit cells. Each flat side of the large hexagon in Figure 2 (left) corresponds to one sector of the model. Each sector consists of 11 rings of coolant channels, 9 of which contain heater rods.

Rings 4-7 consist only of large coolant channels. Rings 1, 2, 9, 10, and 11 contain small coolant channels, and rings 1-3 and 8-11 contain medium coolant channels, as defined in Table I. In the new model, the hydraulic diameter and junction diameter for the pipes representing rings with multiple coolant channel sizes are calculated using the definition of hydraulic diameter, as shown in equation 1, where D_h is the hydraulic diameter, A is the total coolant flow area, and P is the wetted perimeter.

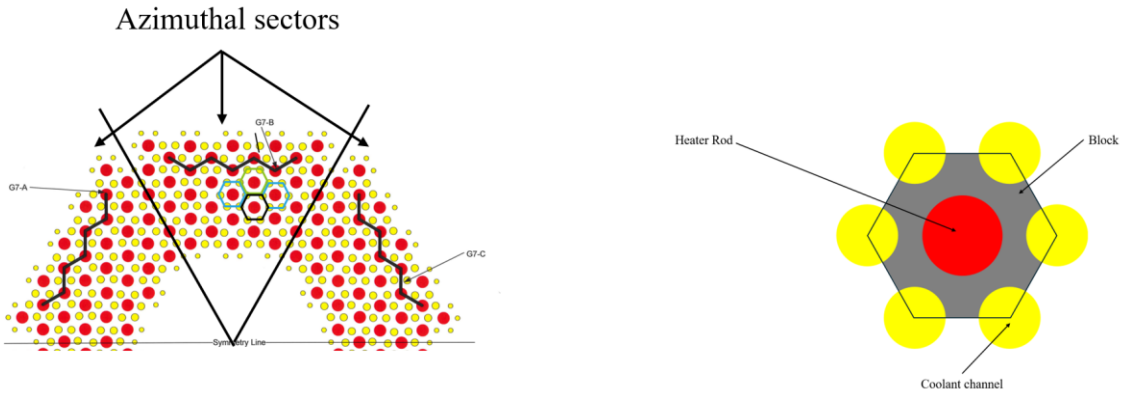

Figure 2. (Left) Whole-core view. The different hexagon colors indicate different "rings" in the core. (Right) Hex block unit cell

$$D_h = \frac{4A}{P} \qquad (1)$$

An additional pipe component is defined for each unit cell to represent the helium gap between the block and the heater rod. This pipe component contains stagnant helium because there is no flow in the gap. In steady-state, these pipes are connected to a time-dependent volume whose pressure and temperature match those of the upper plenum. During a transient, the time-dependent volumes and the junctions connecting them to the gaps are deleted to allow for dynamic behavior in these channels.

2.2. Heat structures

The heat structures in the new model are similar to those in the legacy model. Figure 3 shows the heat structure unit cells from the legacy model. The basic heat structure design for the new model is the same, with heat structures centered on coolant channels and heater rods radiating to the outer surface of the core block unit cell. The specific dimensions, however, differ.

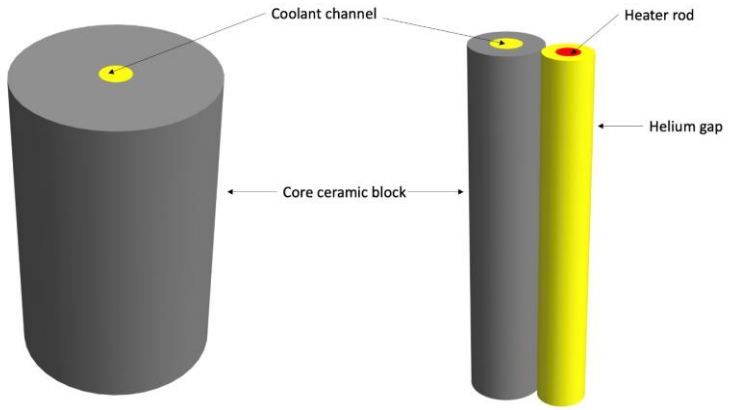

Figure 3. Heat structures unit cell view. The left is the inner reflector unit cell, and the right is the core unit cell.

In the legacy model, the inner reflector was divided into 3 pieces: the inner cylinder, the coolant channel unit cell, and the outer cylinder. In the new model, the inner reflector is just 2 pieces: the inner cylinder and the coolant channel unit cell. The coolant channel unit cell represents the inner reflector coolant channels and the region between the coolant channel and the inner edge of the core, while the inner cylinder represents the reflector in the core center up to the coolant channels. The outer reflector is also composed of just 2 pieces. The inner piece of the outer reflector represents the outer reflector coolant channels, and the outer piece of the outer reflector represents the outer portion of the core block beyond the coolant channels. The legacy model includes a gap between the outer reflector and the permanent reflector. Reviewing the latest core drawings, we could not identify a gap between the outer and permanent reflectors; so instead of modeling a gap with radiation heat transfer across it, the two reflectors are treated as being in contact with each other with conduction heat transfer between them. The radiation heat transfer from the permanent reflector to the barrel, the vessel, and ultimately the RCCS remains unchanged from the legacy model. Figure 4 shows some of the conduction heat transfer paths in the core. To keep the figure easily readable, not all heat structures are shown. The central piece of the inner reflector is shared between the sectors, allowing for conduction between the sectors through the middle of the core. Each sector of the core can transfer heat with the adjacent sectors through conduction enclosures, and heat moves radially through the facility through conduction enclosures as well. Conduction is modelled through conduction enclosures, where each hex unit cell is allowed to conduct to the hexes that surround it, and each sector is allowed to communicate with its neighboring sectors.

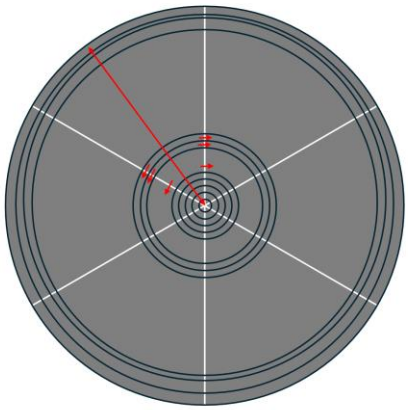

Figure 4. Sample of conduction heat transfer paths from a single sector. Note that several heat structures are not shown in the middle region

3. RESULTS

Due to the different nodalizations in the models, a direct comparison of temperatures at specific (r,z) coordinates is challenging. The axial locations within the core have been preserved, because in both models the axial nodalization in the core is such that each node represents the height of an HTTF core block. We can, thus, compare the temperature distribution at each axial location. We can also compare both models' maximum block temperatures during a PCC. We first present results from a full-power steady state followed by results from a PCC.

3.1. Full-power steady state

The full-power steady state models developed here provide solutions for exercises in two of the HTGR T/H benchmark problems [2]. The full-power steady state boundary conditions can be seen in Table 2. Note that HTTF has a gap between the core vessel and the RCCS panels. That gap is not airtight, and the benchmark specifications include 25 g/s of air flow in that gap during the code-to-code comparison problems. Table 3 shows a comparison of energy balance results in the models. This is a partial comparison that does not include heat lost through the top and bottom heads of the pressure vessel. The primary coolant removes 1.5 kW more power in the new model than it does in the legacy model, and the RCCS water removes 0.1 kW more heat, though when rounding RCCS temperatures to the nearest tenth of a degree, the difference is unidentifiable. These differences are quite small, but they likely arise due to some differences in radiation heat transfer in the models. In the legacy model, heat radiates from the upper reflector to the upper head and from the lower reflector to the solid structures in the lower plenum. These radiation pathways are neglected in the new model; thus, there is slightly more heat that can be removed by the primary coolant.

A comparison of the helium and block temperatures at blocks 1, 3, 5, 7, 9, and the top of the lower reflector (LR 3) in the core region can be seen in Figure 5. The 10 blocks in HTTF are numbered from the bottom up, so block 1 is at the bottom of the core. The temperatures shown in the figure correspond to the top of the blocks – a location that was chosen based on the presence of thermocouples for validation in later modeling activities. Both block and helium temperatures in the new model show a spike at the second and tenth rings. This spike occurs because rings 2 and 10 contain small and medium coolant channels and heater rods. Rings 1 and 11 contain small and medium coolant channels but do not contain heater rods; hence, the lower temperatures in those rings. Moving towards the middle of the core region, only large coolant channels are present, so there is a greater

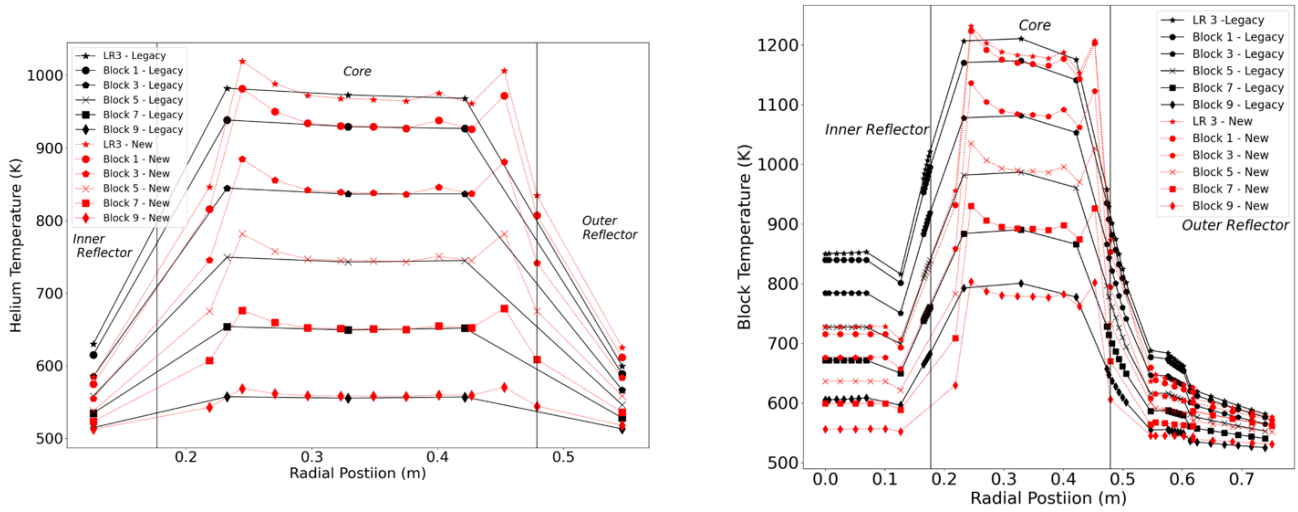

Figure 5. Helium (left) and block (right) temperatures in steady state.

Table II: Full-power steady state boundary conditions

Parameter	Value
Power (MW)	2.2
Helium Flow Rate (kg/s)	1.0
Helium Inlet Temperature (K)	500.0
Helium Pressure (MPa)	0.7
RCCS Water Flow Rate (kg/s)	1.0
RCCS Water Inlet Temperature (K)	313.2
RCCS Water Pressure (MPa)	0.1
RCCS Cavity Air Flow Rate (kg/s)	0.025
RCCS Cavity Air Inlet Temperature (K)	300.0

Table III: Energy balance comparison between the old and new models in full-power steady state.

	Power Removed by Helium (kW)	Power Removed by Cavity Air (kW)	Power Removed by RCCS (kW)	Helium Outlet Temperature (K)	RCCS Outlet Temperature (K)
Old Model	2185.2	1.5	12.4	921.2	316.2
New Model	2186.8	1.5	12.5	921.7	316.2

coolant flow rate in that region, and the lower local power-to-flow ratio means lower temperatures. Temperatures in the inner reflector are considerably lower in the new model than in the legacy model, but temperatures in the core and in the outer and permanent reflectors are similar. Temperature differences in the inner reflector range from -48 to -119 ΔK at the center of the core to -10 to +1 ΔK at the outer edge of the core. In the core region, the temperature peaks in the new model can be up to 60 ΔK hotter than the closest temperature in the old model, and the temperature valleys can be as much as 23 ΔK colder than the closest temperature in the old model. The temperatures near the middle of the core region are anywhere from 3-23 ΔK below those in the old model.

The steady-state results from the new model show temperatures in the inner reflector that range from 8-15% lower than the legacy model relative to the values from the legacy model; temperatures in the core region can range from 2 % lower to 8% higher than similar temperatures in the legacy model; though those temperature comparisons do not correspond to the exact same volumes. Temperatures at the edge of the core range from 1.7% lower to 1.0% higher in the new model.

3.2. Pressurized conduction cooldown transient

The PCC is a transient that occurs when forced circulation of the coolant stops but the coolant pressure boundary remains intact. In this instance, the PCC is initiated by ramping the coolant inlet flow down from 1.0 kg/s to 0.0 kg/s linearly over 1 second. Decay heat is simulated using the ANS-94 decay heat standard for the sake of the code-to-code comparison exercises. Following cessation of forced circulation and the switch to decay heat mode, the PCC can be divided into three distinct phases: rapid heatup of the core, temperature redistribution, and long-term cooldown. In this case, the first phase occurs relatively quickly, over the span of a few minutes. The second phase occurs over a period of a few hours, as the core region begins to cool down by conducting heat to both the inner and outer reflectors. During this phase, intracore natural circulation may be established. Intracore natural circulation can redistribute heat from the hottest parts of the core (near the bottom) toward the cooler parts of the core (near the top), but it does not remove heat from the system. This second phase ends when the temperature in the inner reflector peaks. The final phase, long-term cooldown, occurs over a period of tens of hours.

We simulated the PCC for 48 hours, at which point the coolant exit temperature of the RCCS had already peaked, and the entire system was cooling down. For the PCC, we compared the peak block temperature between the two models. Figure 6 shows the peak value of block volume-averaged temperature over time from all the block heat structures in both models. The change in slope of the peak temperature at approximately 3.5 hours in the legacy model and 6.25 hours in the new model occurs because the hottest location is changing. During steady-state operation, the core region is the hottest part of the system, but as the heat is redistributed inward, the core and the inner reflector reach an equilibrium, causing the core to conduct heat only outward. At this point in time, the inner reflector becomes the hottest part of the system. The change in slope occurs as the temperature of the inner part of the inner reflector overtakes that of the core region.

In the legacy model, the maximum temperature reached in the block, including the inner reflector, core region, outer reflector, and permanent reflector was 1,233.7 K. In the new model, the peak temperature is 1,243.4 K. The difference between the two is 10 K. The peak steady-state block temperature in the new model is 1233.3 K, and in the old model it is 1210.5 K. This means that the temperature rise in the new model, from steady state to maximum, is 5.3 K. The temperature rise in the old model is 23.2 K. After the first hour, the temperatures of the old and new models begin to diverge. The increased thermal resistance leads to lower steady-state temperatures in the inner reflector shown in Figure 6, and because the inner reflector is the hottest point in the facility during most of the PCC, the higher thermal resistance moving inward leads to more heat flow outward and therefore the faster reduction in peak temperature for the new model, but this is not enough to explain the differences in results. While steady-state RCCS heat removal is slightly greater in the new model than the legacy model, the transient RCCS heat removal is lower. This may be a result of the elimination of the gap between the outer reflector and the PSR. It may be a result of new conduction enclosures having greater thermal resistance than the old ones, or it may be the result of something that we have yet to identify.

Intracore natural circulation is an important phenomenon in the PCC, but the relatively low pressure of HTTF leads to relatively small amounts of natural circulation. Following the cessation of forced flow, hot helium at the bottom of the core begins to rise. In the top plenum, helium from each channel mixes, and ultimately, a loop forms where coolant in the inner reflector and inner parts of the core flows upward while coolant in the outer parts of the core and the outer reflector flows downward and helps redistribute heat

towards the top and edge of the system. The natural circulation flow rate is defined as the sum of the flow in all the channels in downflow at 48 hours. In the legacy model, the natural circulation flow rate was 0.3 g/s, but in the new model, it is 0.2 g/s. In the legacy model, upflow occurs in the inner reflector, the inner core ring, and the middle core ring. The outer core ring and outer reflector are in downflow. In the new model, upflow occurs in the inner reflector and rings 1 through 8, while rings 9-11 and the outer reflector are in downflow. The flow patterns are similar, but the difference in magnitude of the flow rate is 1/3 of the flow rate in the old model; however, the difference is just 0.1% of the forced flow rate.

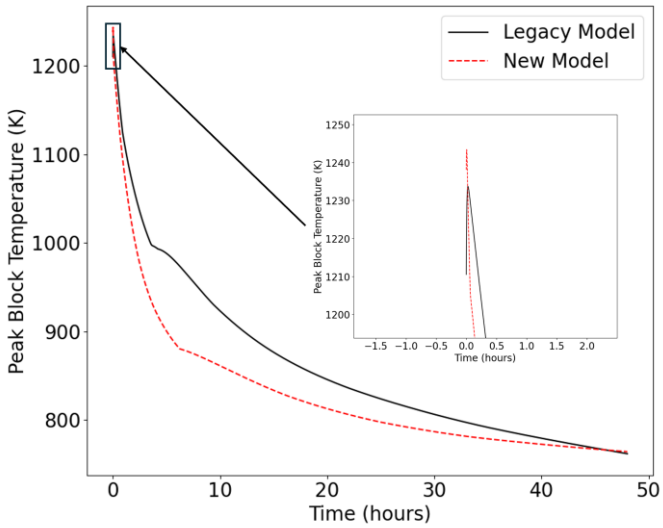

Figure 6. Comparison of the legacy and new models in terms of peak temperature over time in the PCC

The new model shows similar trends in both peak temperature and natural circulation as the legacy model during a PCC. The difference in maximum temperature is just 10 K, but differences in peak temperatures grow over time until the slope of peak temperature changes in the new model at approximately 6.25 hours. Following that, the peak temperatures begin to converge.

4. CONCLUSIONS

In this paper we have presented the development of a new RELAP5-3D model for HTTF and compared results between the legacy model and the new model for a full-power steady state and for a PCC initiated from full-power steady state. The new model divides the core into 6 azimuthal sectors and increases the number of radial nodes within the core region from 3 to 11. This more finely nodalized model was developed for modeling HTTF experiments such as PG-27 and PG-29 which have radially non-uniform power distributions, and in the case of PG-29 an azimuthally asymmetric power distribution too. We will investigate these transients in the future. The comparison presented in this paper of the two models for full-power steady state provides a base line using conditions that both models are capable of representing well.

The steady-state block and helium temperatures are very similar between the two models, with the exception of temperatures in the inner reflector. In the inner reflector, the block temperatures are 48-119 K lower in the new model than the old. During the PCC, the maximum block temperature from the entire transient predicted by the two models differs by just 10 K, and the temperature rise differs by 17.9 K. These differences are quite small. Over time, the difference in peak temperature grows, as the new model shows a lower peak temperature than the old model. These differences are under investigation, and until validation

studies with the new model are completed, we cannot say with certainty which set of results is correct. The natural circulation flow rates and patterns are similar between the old and new models. The same flow pattern develops, and the difference in natural circulation flow rate is just 0.1 g/s.

Overall, the two models show similar results for the steady state and the PCC, but with slower heat removal during the PCC in the new model. A few differences arise due to the differences in nodalization between the models or due to differences in conduction enclosures between the two models. The results of this comparison provide confidence that we can move forward with modeling of HTTF scenarios where the finer nodalization of the new model has an opportunity to demonstrate significant benefits over the relatively coarse nodalization of the old model. Validation work based on the new model is ongoing and will provide further insight into RELAP5-3D capabilities for HTGR thermal hydraulics modeling.

ACKNOWLEDGMENTS

This work was funded by the U.S. Department of Energy (DOE) Advanced Reactor Technologies Gas-Cooled Reactor (ART-GCR) program. This research made use of the resources of the High Performance Computing Center at INL, which is supported by the DOE Office of Nuclear Energy and the Nuclear Science User Facilities under contract no. DE-AC0705ID14517.

This manuscript was authored by Battelle Energy Alliance, LLC, under contract no. DE-AC07-05ID14157 with DOE. The U.S. Government retains and the publisher, by accepting the article for publication, acknowledges that the U.S. Government retains a nonexclusive, paid-up, irrevocable, worldwide license to publish or reproduce this manuscript or allow others to do so for U.S. Government purposes.

REFERENCES

1. D. G. Petti, J. Gehin, H. Gougar, G. Strydom, T. O'Connor, F. Heidet, F., J.Kinsey, C. Grandy, A. Qualls, N. Brown, J. Powers, E. Hoffman, and D. Croson, "A Summary of the Department of Energy's Advanced Demonstration and Test Reactor Options Study," *Nuclear Technology,* **199**, pp. 111–128 (2017). doi: https://doi.org/10.1080/00295450.2017.1336029
2. A. S. Epiney et al., "Overview of HTTF Modeling and Benchmark Efforts for Code Validation for Gas-Cooled Reactor Applications," *Prroceedings of the Fourth International Conference on Generation IV & Small Reactors (G4SR-4)*, Toronto, ON, Canada, October 3–6, 2022, 2022.
3. P. Bayless, "RELAP5-3D Input Model for the High Temperature Test Facility," Idaho National Laboratory, Idaho Falls, ID, USA, INL/EXT-18-45579 (2018).
4. A. S. Epiney, "RELAP5-3D Modeling of High Temperature Test Facility Test PG-26," Idaho National Laboratory, Idaho Falls, ID, USA (2020). https://doi.org/10.2172/1676420
5. A. Gairola and A. S. Epiney, "RELAP5-3D Simulation of Pg-27 Test at the HTTF," Idaho National Laboratory, Idaho Falls, ID, USA, INL/EXT-21-63798 (2021).
6. R. F. Kile, A. S. Epiney, and N. R. Brown, "High Temperature Test Facility sensitivity and calibration studies to inform OECD-NEA benchmark calculations," *Nuclear Engineering and Design,* **404** (2023). doi: 10.1016/j.nucengdes.2023.112178
7. J. Halsted and I. Gutowska, "Verification and validation of a lower plenum mixing test at the OSU High Temperature Test Facility," *Nuclear Engineering and Design,* **406**,pp. 112251 (2023). doi: 10.1016/j.nucengdes.2023.112251.
8. R. F. Kile, A. S. Epiney, and N. R. Brown, "RELAP5-3D Validation Studies based on the High Temperature Test Facility," *Nuclear Engineering and Design,* **426** (2024). doi: 10.1016/j.nucengdes.2024.113401.
9. I. Gutowska, B. Woods, "OSU High Temperature Test Facility Design Technical Report," Oregon State University, Corvallis, Oregon, OSU-HTTF-TECH-003-R2 (2019).